CellR4 2015; 3 (1): e1401

# Understanding the bioactivity of stem cells seeded on extracellular matrix scaffolds produced from discarded human kidneys: a critical step towards a new generation bio-artificial kidney

*A. Petrosyan[1], G. Orlando[2,3], A. Peloso[2,4], Z. Wang[2], A.C. Farney[2], J. Rogers[2], R. Katari[2,3], S. Da Sacco[1], S. Sedrakyan[1], R.E. De Filippo[1], R.J. Stratta[2], S. Soker[3], L. Perin[1]*

[1]GOFARR Laboratory, Saban Research Institute, Children's Hospital Los Angeles; Department of Urology, University of Southern California, Los Angeles, CA, USA.

[2]Department of General Surgery, Section of Transplantation, Wake Forest School of Medicine, Winston Salem, NC, USA

[3]Wake Forest Institute for Regenerative Medicine, Wake Forest School of Medicine, Winston Salem, NC, USA

[4]General Surgery, Fondazione IRCCS Policlinico San Matteo Pavia and University of Pavia, Pavia, Italy

[5]Carolina Donor Services, Winston Salem, USA

Giuseppe Orlando and Astgik Petrosyan share the first Authorship

*Corresponding Authors:* Laura Perin, Ph.D; e-mail: lperin@chla.usc.edu;
Giuseppe Orlando, MD, Ph.D; e-mail: gorlando@wakehealth.edu

**Keywords:** Human renal extracellular matrix scaffolds (hrECM), Human amniotic fluid stem cells (hAFSC), Cell-matrix interactions.

## Abstract

***Background:*** **In the attempt to develop a clinically relevant platform for kidney bioengineering, we have previously demonstrated that human renal extracellular matrix scaffolds (hrECM) can be successfully and consistently produced from discarded kidneys. The hrECM are shown to maintain intricate architecture of macromolecules and vasculature. One of the main roadblocks in the bioengineering of transplantable kidneys is the incomplete understanding of how the extracellular matrix influences cellular behavior and response.**

***Materials and Method:*** **In the present study, we established a 3D in vitro model useful to investigate the interactions between stem cells and the extracellular matrix. Human amniotic fluid stem cells (hAFSC) were seeded on multiple samples of hrECM and cultured for up to 6 weeks. Histological examination of seeded scaffolds, analysis of secretomes, cell viability assessments, and PCR were carried out at different time points.**

***Results:*** **We observed that hAFSC attach and proliferate when seeded on the matrix. hAFSC synthesize and secrete various chemokines and growth factors involved in angiogenesis (VEGF, TGF-alpha, IL-8) and inflammation, as well as mediators of matrix remodeling (MMP-2, TIMP-2). Ultrastructure analysis of cell-matrix interaction identified variation in cellular morphology based on renal compartment localization. Early kidney developmental markers, PAX and LIM1B, were expressed after 2 weeks of culture by hAFSC.**

***Conclusions:*** **These results suggest that hrECM seeded with hAFSC behave as an effective and viable biosystem. Furthermore, this in vitro model may be used to study cell-matrix interactions and the mechanisms of tissue regeneration or repair occurring in the kidney.**

## Introduction

Despite significant advances in transplantation surgery, a limited supply of transplantable kidneys has increased the mortality of patients on waiting lists[1]. The ideal scenario in all of organ transplantation is one involving an inexhaustible source of transplantable tissues without the need for immunosuppression[2]. Recently, seminal advances in organ bioengineering and regeneration have allowed for the production and implantation of several different constructs including bone, cartilage, skin, the cornea, vessels, the vagina, and segments of the urinary tracts and upper airways in more than 200 patients[1]. Importantly, no immunosuppression was

administered at any time post-transplantation because these constructs were manufactured from autologous cells in combination with synthetic or natural scaffolds. However, the bioengineering of highly complex organs, such as the kidney, requires the reconstitution of the intricate architecture of macromolecules and vasculature necessary for proper function and survival. Thus, the choice of scaffold is crucial for *ex vivo, in vitro* fabrication.

Extracellular matrix (ECM) scaffolds obtained from organs of human or non-human origin, recapture the complexities absent in their synthetic counterparts[3,4]. In fact, innate ECM produced by resident cells present a vast array of bioactive ECM-bound proteins which modulate cellular adhesion and communication throughout development and disease[5]. Moreover, ECM scaffolds are a biochemically, geometrically, and spatially ideal platform for organ bioengineering. Innate ECM scaffolds retain basic structural proteins and polysaccharides, matrix-bound growth factors, and cytokines[6,7]. Furthermore, they exhibit an intact and patent vasculature capable of sustaining physiologic blood pressure when implanted *in vivo*[8]. Underscoring the potential of these scaffolds, ECM is able to drive differentiation of progenitor cells into an organ-specific phenotype[9-12].

We have previously demonstrated that human renal ECM scaffolds (hrECM) can be produced successfully and consistently from kidneys initially procured for transplantation but eventually discarded due to severe damage, anatomical anomalies, or excessively long ischemia time[13]. Such hrECM are completely acellular, maintain their architecture and molecular composition, and lack cell membrane molecules such as HLA antigens. Furthermore, hrECM possess remarkable angiogenic properties demonstrated by their ability to induce vessel formation when implanted *in ovo* (chorioallantoic membrane assay)[13]. We assessed the ability of hrECM to sustain cell function and survival by designing an *in vitro* model in which they were seeded with human amniotic fluid stem cells (hAFSC). We opted for hAFSC due to their remarkable ability to modulate important molecular pathways which come into play during kidney disease progression, in both acute and chronic models[14-16]. The present study showed that hrECM seeded with hAFSC behave as an efficient "biosystem" in which cells adhere and proliferate within the framework of the matrix. Cellular activity evaluated via proteomic analysis demonstrated that seeded cells have the ability to secrete numerous cytokines, chemokines and growth factors involved in critical pathways, like inflammation, angiogenesis and matrix turnover and remodeling.

## Materials and Methods

### Procurement, preparation and decellularization of discarded human kidneys

To obtain hrECM, we used renal grafts procured within the designated service area of our local organ procurement organization (Carolina Donor Services) and of the organ procurement organization in Charlotte, NC (LifeShare of the Carolinas). In all cases, organs were refused by all local, regional, and national transplant centers. After exhaustion of the national list, kidneys from donors with research consent were offered for research purposes to the transplant team of Wake Forest School of Medicine and processed at the Wake Forest Institute for Regenerative Medicine. The study was approved by the IRB of the Wake Forest School of Medicine and kidneys were prepared and processed as previously described[13]. For the specific purposes of the present study, we added two steps to additional steps. First, after decellularization with SDS (USB Corporation, Cleveland, OH, USA), 1000 mL of DNase solution (0.0025 w/w% DNase (Sigma-Aldrich, St. Louis, MO, USA DN25) and 10 mM magnesium chloride (Sigma-Aldrich, St. Louis, MO, USA M4880) in 1× PBS at neutral pH) was circulated through the hrECM overnight to allow digestion of residual DNA; thereafter, hrECM were rinsed with PBS for 5 days at a flow rate of 6 mL/min (43,320 mL total). The so-obtained hrECM were stored in PBS. Subsequently, hrECM were irradiated with cobalt gamma (JL Shepherd and Associates, Inc., San Fernando, CA, USA) at a dose between 20 to 25 kGy for 6-8 hours, depending on the scaffold size, with a temperature of 20°C to achieve sterilization.

### Isolation, culture, and labelling of hAFSC.

Discarded samples of human amniotic fluid from male fetuses (12-20 weeks of gestation) were provided to our laboratory at Children's Hospital Los Angeles by Labcorp (Monrovia, CA, USA). IRB exemption was obtained since no written or verbal consent was required as samples were not identified. Cells were isolated and characterized as pre-

viously described[14-16]. Briefly, hAFSC were positively selected for the surface marker c-kit (Santa Cruz Biotechnology, Dallas, TX, USA) by magnetic activated cell sorting (MACS, Miltenyi Biotech, Auburn, CA, USA), cloned and cultured in Petri dishes in Chang medium composed of α-MEM, 20% Fetal Bovine Serum, 1% L-Glutamine and 1% antibiotics (pen-strep) (Gibco/BRL, Rockville, MD, USA) supplemented with 20% Chang Medium B and 2% Chang Medium C (Irvine Scientific, Santa Ana, CA, USA).

The selection of c-kit positive cells from the total population of amniotic fluid cells using the MACS/FACS techniques is very well established in our laboratory. C-kit positive cells are shown to be pluripotent, they do not form teratoma *in vivo*, they can be easily cloned and expanded without any genetic transformation and they present maintenance of normal karyotype[14-17]. Most importantly, we have established that these cells are able to protect organs from damage in animal models of acute and chronic renal and lung failure, and diabetes[15-16,18-20]. Therefore, in order to be consistent with our previous experiments and publications, in this Manuscript we used the same cloned-c-kit population we have deeply characterized as a new platform to study stem cells – ECM interaction.

For labelling experiments, hAFSC were detached using trypsin (Life Technology, Grand Island, NY, USA), counted, and re-suspended for 5 min at 37°C in a solution of 500 $\mu$l of PBS (Gibco/Invitrogen, Carlsbad, CA, USA) and 10 $\mu$l of cell surface marker CM-Dil (Invitrogen, Carlsbad, CA, USA). They were then held at 4°C for 15 min before being washed twice with PBS and then seeded on hrECM.

### Seeding of hAFSC on hrECM.

An approximately 1.8 cm diameter section was cut from hrECM and then cross-sectioned to a thickness of 300 $\mu$m using a vibratome (Leica, VT1000S Vibratome). Cross sections were reduced to approximately 1 cm$^2$ in size. These sections were stored for up to 2 weeks in a solution of PBS with 2% pen/strep and 0.02% Primocin (InvivoGen, San Diego, CA, USA). Prior to cell seeding, matrices were washed in PBS for 2 hours followed by FBS (Gibco/BRL, Rockville, MD, USA) for 2 hours at 37°C. 1x10$^6$/cm$^2$ CM-Dill labelled hAFSC next underwent 24 hrs of static seeding at 37°C in 5% $CO_2$ using 500 µl of Chang's media in 25 cm$^2$ ultralow attachment culture flasks (Corning, Inc., Tewksbury, MA, USA). After 24 hrs, 5 ml of Chang's media was added and changed every 48 hrs. In addition, after 3 days of static seeding samples were placed on an orbital shaker at 110 rpm, at 37°C in 5% $CO_2$, for the remaining time of the culture. Fifteen culture flasks each containing 6 sections were used to collect data. Three to 7 randomly selected samples were collected for histology on each of time point (days 14, 28 and 35). Eighteen randomly selected sample sections were collected for PCR on each of days 14 and 28.

### Fixation and Histology

Acellular hrECM and hrECM seeded with hAFSC were fixed in 10% formalin (Azer Scientific, Morgantown, PA, USA) for 2 hrs. After fixation, samples were dehydrated in alcohol gradients and placed in toluene (Sigma-Aldrich, St. Louis, MO, USA) for 30 min. Samples were kept overnight in a 50:50 toluene paraffin mixture. They were next moved into paraffin for 2 hrs and later embedded. 5 µm thick sections (Rotary Microtome-Leica, Rotary Microtome *RM2235)* were deparaffinized and rehydrated in alcoholic gradients for histology. Haematoxylin and eosin (Sigma-Aldrich, St. Louis, MO, USA) staining was performed by 90 seconds of incubation in haematoxylin followed by 30 seconds of incubation in eosin. Sirius Red/Fast Green FCF (Sigma-Aldrich, St. Louis, MO, USA) staining was performed with 1 hr of incubation in Sirius Red solution and a 2 min wash in 0.1N hydrochloric acid (Sigma-Aldrich, St. Louis, MO, USA). Trichrome Masson staining samples were fixed with Bouin's Solution (Sigma-Aldrich, St. Louis, MO, USA) for 15 min at 56°C followed by Wiegerts iron haematoxylin (Sigma-Aldrich, St. Louis, MO, USA) for 5 min, then a trichrome Kit (Sigma-Aldrich, St. Louis, MO, USA), and finally incubated with 1% acetic acid (Sigma-Aldrich, St. Louis, MO, USA) for 2 min. A bright field microscope was used to take 20x images. DAPI mounting (Vector Laboratories Burlingame, CA, USA) was used to visualize hAFSC seeded on hrECM with a Leica DM5500 B Microscope System.

### Immunohistochemical (IHC).

IHC analysis of apoptosis and proliferation was conducted by 1-hour incubation with primary antibodies PCNA (ABCAM, Cambridge, MA, USA 1.5:1,000) and Bcl-associated X protein (Bax) (Santa Cruz Biotechnology, Dallas, TX, USA 1:100), followed by 30 minute incubation with Immune Pres Reagent

Kit Anti-Rabbit (Vector Laboratories Burlingame, CA, USA). Samples were visualized with Impact DAB Kit (Vector Laboratories Burlingame, CA, USA) followed by counter-staining with haematoxylin. A minimum of 30 20x bright field microscopic images (Leica DM 1000) per time point were counted for positive expression of PCNA and Bax. ImageJ software determined cell count.

### PCR

RNA was extracted from hAFSC cultured on petri dishes (control before seeding) and hAFSC seeded on hrECM at 14 and 28 days. RNA was also extracted from un-seeded hrECM as a control. mRNA for PCR analysis of seeded and un-seeded hrECM at 14 and 28 days in culture was collected from represent pooled samples, n=6. All RNA extractions were conducted using the Qiagen RNeasy kit (Qiagen, Valencia, CA, USA) according to the manufacturer's instructions. PCR was performed under 40 Cycles with REDTaq® ReadyMix™ PCR Reaction Mix (Sigma-Aldrich, St. Louis, MO, USA) using an Eppendorf AG 22331 (Eppendorf, Hamburg, Germany). Genes tested along with primer sequences are listed in Table 1. PCR was performed in triplicate for all experimental groups and visualized by 2% Agarose Gel (EMD Millipore. Billerica, MA, USA).

**Table 1.** List of human primers used in the experiments

| GENE | Primer sequence (5'→3') |
|---|---|
| GDNF (617bp) | TATGGGATGTCGTGGCTGT<br>ACACCTTTTAGCGGAATGCTT |
| β-actin (395bp) | AGAAAATCTGGCACCACACC<br>CTCCTTAATGTCACGCACGA |
| LMX1B (627bp) | AAGAGCGAGGATGAAGATGG<br>TCAGGAGGCGAAGTAGGAAC |
| PAX-2 (738bp) | AGGATGAGGGACCAACTGC<br>AACGACAGAACCCGACTATGTT |
| Nephrin (568bp) | ACACGGAGCACACATACCAC<br>ATTGGAGAGGAGCAGAAG |
| WT1 (131bp) | GAGAGCCAGCCCGCTATTC<br>CATGGGATCCTCATGCTTG |
| PODXL2 (187bp) | TACGCAGGTGATCTGCAAGG<br>GCTCAGAGAGATGTGCCAGG |
| VEGFA (124bp) | GCGGAGAAAGCATTTGTTTGT<br>CGGCTTGTCACATCTGCAA |
| SYNPOL2 (619bp) | TGGGGACACTGTTCAAACTCC<br>GAGGGCCAGGGATAGTAGGT |

### Luminex Analysis

Secretion of matrix metalloproteases (MMPs), tissue inhibitor of metalloproteases (TIMPs), cytokines, growth factors, and interleukins was determined in hAFSC prior to and throughout seeding on hrECM. At days 4, 7, 14, and 28, a minimum of 3 samples of media was collected and protein concentration measured using DC™ Protein Assay (Bio-Rad Laboratories Hercules, CA, USA). Expression of the proteins was assessed using MILLIPLEX MAP Human Cytokine/Chemokine Magnetic Bead Panel-Premixed 42 Plex, MILLIPLEX MAP Human MMP Magnetic Bead Panel 2, and MILLIPLEX MAP Human TIMP Magnetic Bead Panel 2 (EMD Millipore, Billerica, MA, USA) according to the manufacturer's instructions and analysed using the Luminex Multiplex System (EMD Millipore, Billerica, MA, USA).

### Transmission Electron Microscopy (TEM)

hrECM seeded with hAFSC and cultured for 28 days (n=3) were fixed with 2% glutaraldehyde (Sigma-Aldrich, St. Louis, MO, USA) in sodium phosphate buffer. Samples were then placed in 1% osmium tetroxide (Sigma-Aldrich, St. Louis, MO, USA) for 1 hour and dehydrated in 50%, 70%, 90%, 95%, 100%, ethanol and propylene oxide (Sigma-Aldrich, St. Louis, MO, USA) for 10 min each. Samples were then infused with an epoxy resin mixture (Eponate 12 resin) (TED PELLA Inc. Redding, CA. USA). Ultra-thin sections were collected on copper grids (Electron Microscopy Science. Hatfield, PA, USA), and sections were stained using 10% uranyl acetate (Electron Microscopy Science. Hatfield, PA, USA) in 50% methanol (Thermo Fisher Scientific, Waltham, MA, USA) and a modified Sato lead stain (Pathology Laboratory, Children's Hospital Los Angeles, LA, USA). A Morgagni 268 electron microscope (FEI, Hillsboro, OR, USA) was used for picture acquisition with the assistance of the Pathology Laboratory, Children's Hospital Los Angeles.

### Statistical Analysis.

Results are presented as mean ± SEM. Data were tested for normality using the Shapiro-Wilk test. Statistical differences between groups were determined using unpaired *t* test (Figure 1), repeated measures ANOVA (Figures 2, 3 and 4; Table 2) as appropriate. Non-parametric data were analysed using Kruskal-Wallis one-way ANOVA on Ranks. A Holm-Sidak post-hoc test was used for multiple

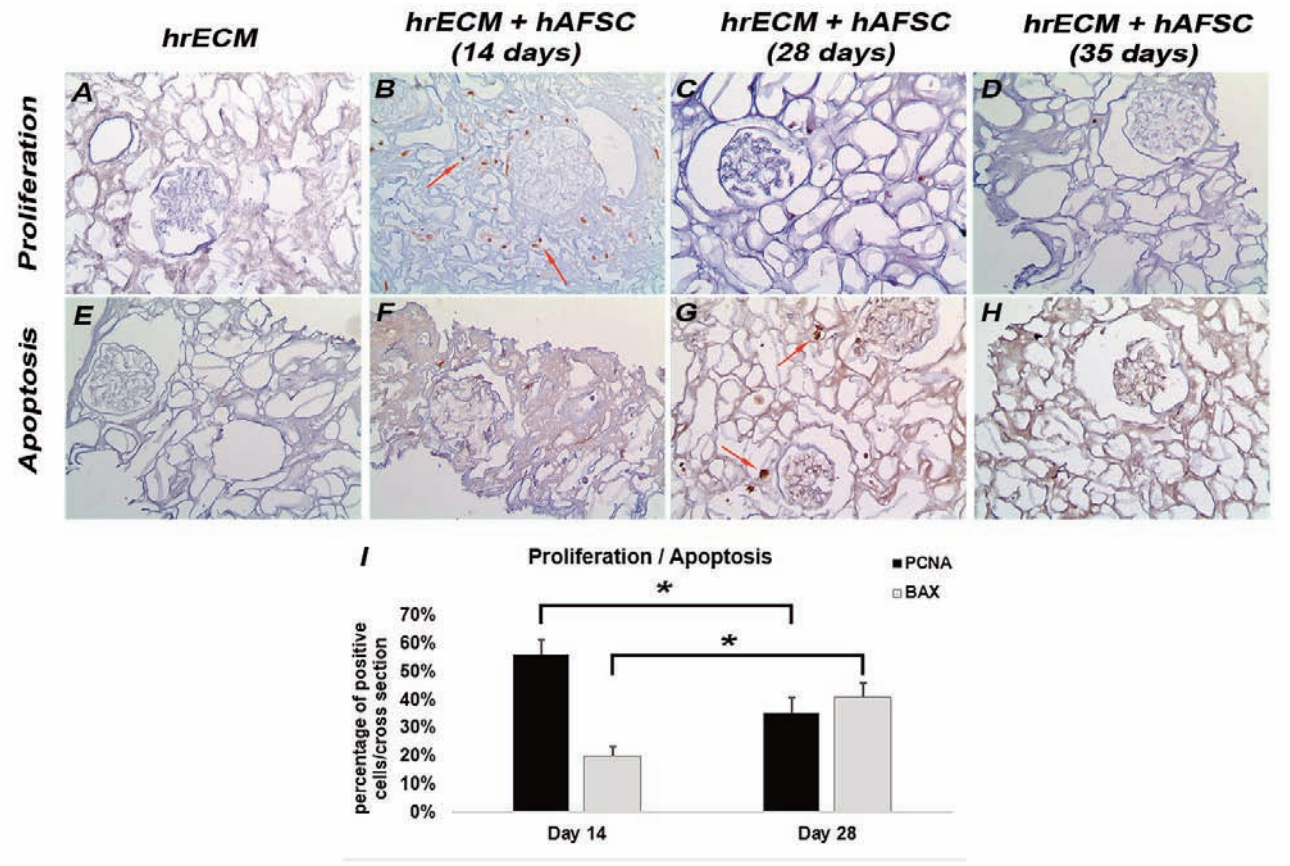


**Figure 1.** hAFSC proliferation and apoptosis after seeding on human renal extracellular matrix (hrECM) at day 14, 28 and 35. PCNA *(B-D)* and BAX *(F-H)* staining for hAFSC seeded on hrECM at 14, 28 and 35 days. At day 14 it is evident an increase of proliferation (*B*, *arrow*) compared to apoptosis *(F)*. In Figure *A* and *E* is represented hrECM alone and no expression of BAX or PCNA is present. I. Graph showing the quantitative expression of PCNA and BAX at different time points after seeding (**p*<0.05). A-H: scale bar: 100 μm.

comparisons when appropriate. A *p* values less than or equal to 0.05 were considered significant and expressed as **p*<0.05; ***p*<0.001.

## Results

### hAFSC-hrECM interaction (Figure 5).

In order to investigate whether hAFSC attach throughout the hrECM, H&E (A-D), Sirius Red (E-H), Masson Trichrome (I-L) and DAPI (M-P) staining were performed. H&E staining was used to reveal hrECM morphology and in particular of glomeruli, Serious Red and Masson Trichrome were used to identify possible scar formation within the hrECM while DAPI was used to detect cell presence before and after seeding. It is clear that no cells were present within the hrECM before seeding (Figure 1A,E,I) since no cellular staining was detected; these data are also confirmed by absence of DAPI staining as shown in Figure 5M. After seeding, cells attach to the matrix and spread ubiquitously throughout the 3D framework of hrECM as presented in Figure 5B,F,J,N. Moreover, hAFSC labeled with cell surface marker CM-Dil localize near and within large vacant spaces (possibly, capillaries) at 14 days (Figure 5N, *arrow*). 14 days is also the time point in which cells seem to be highly concentrated (Figure 5J,N). By day 28, hAFSC are visually more dispersed and adherent throughout the hrECM (Figure 5H, *arrow*). As expected, our matrices demonstrated histologically significant damage as revealed by the presence of fibrotic scarring; accumulation of collagen fibers is shown by Sirius Red and Masson Trichrome (Figure 5F,J). The presence of this scar tissue is the main reason for discard.

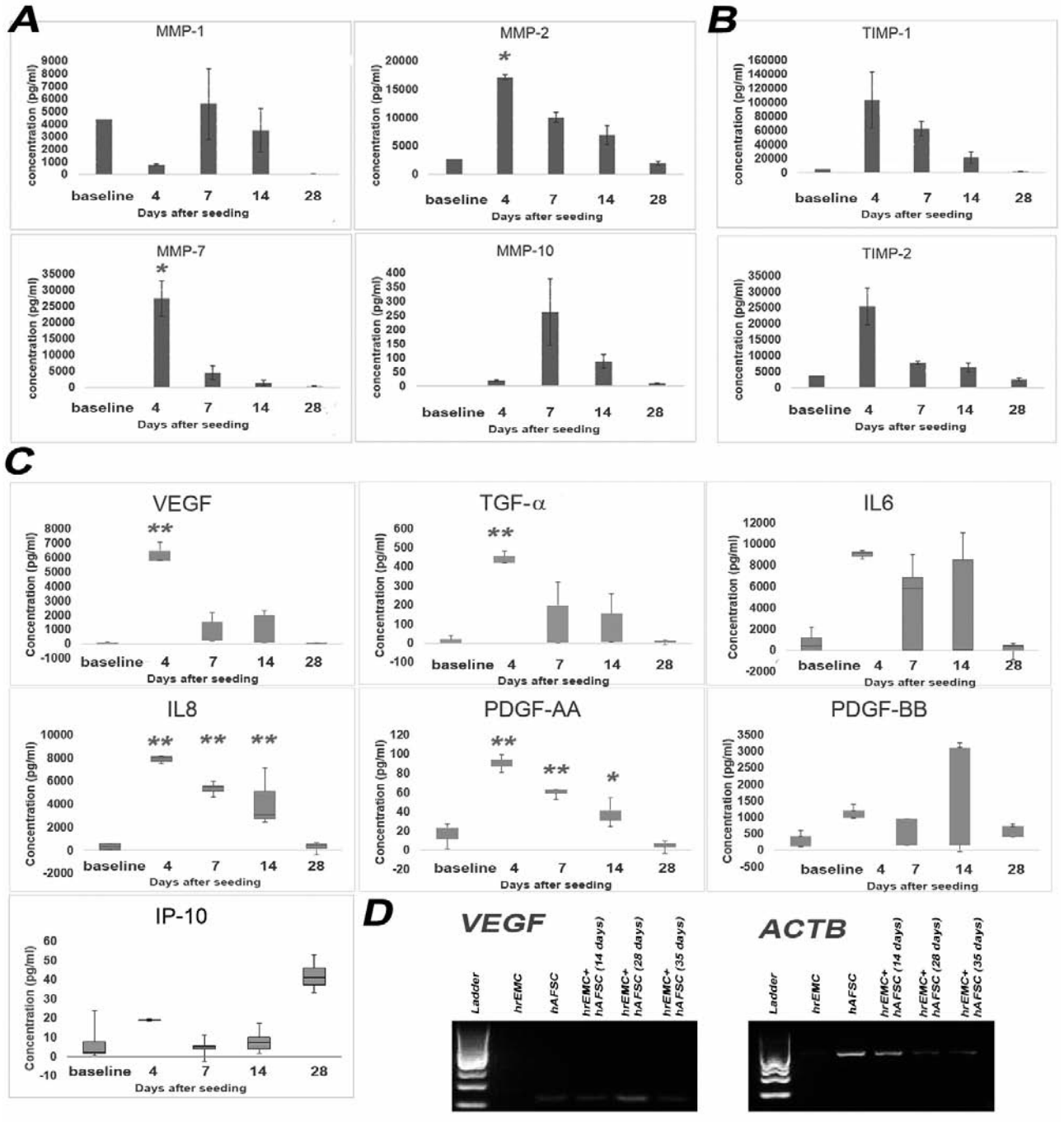


**Figure 2.** Secretome analysis of proteins expressed by hAFSC over 4, 7, 14 and 28 days after seeding on human renal extracellular matrix (hrECM). Comparison of secretome by Luminex analysis of hAFSC before seeding versus hAFSC seeded on hrECM revealed early expression of total (active and inactive) MMP-2 and MMP-7 along with TIMP-1 and TIMP-2. It is evident a significant expression of MMP-2 on days 4 and 7 while TIMP-2 is significantly expressed on day 7 (A, B, Table 2). VEGF, TGF-α, Il-8, PDGF-α and PDGF-β are highly expressed during the first days of seeding. The expression of these proteins is very low when cells are not seeded on the hrECM and cultured in basic media *(C)*. * = $p<0.05$; ** = $p<0.001$. For clarity of the data the multiple comparison between different time points and its statistical significance is reported in Table 2. D. RNA analysis demonstrated expression of VEGFA by hAFSC up to 35 days of culture with a decrease in the expression as time progresses. β-actin is used as housekeeping gene. Media was collected from 3 samples and analysis repeated in triplicate.

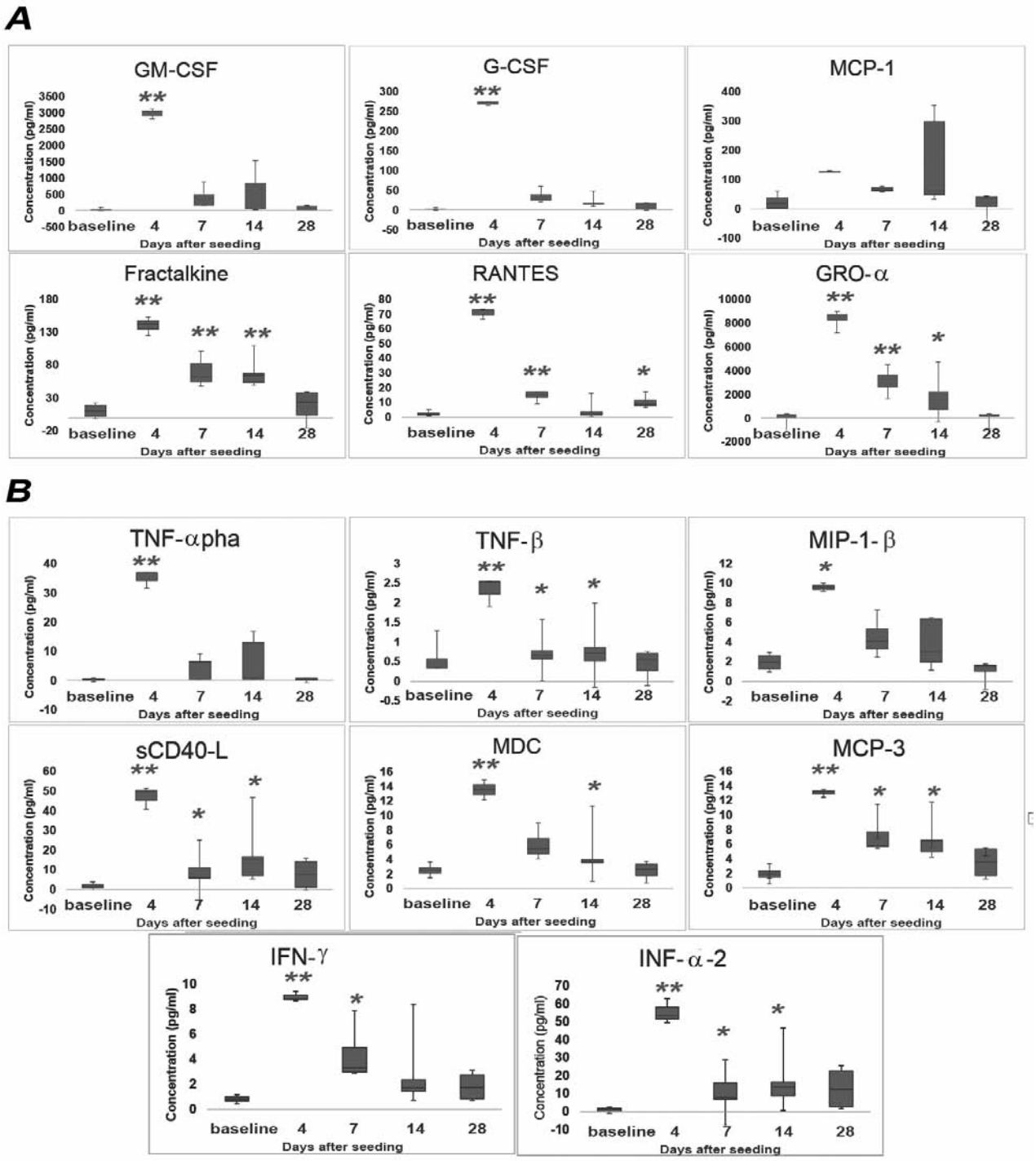


**Figure 3.** Secretome analysis demonstrated secretion of various growth factors and chemokines by hAFSC over 4, 7, 14 and 28 days after seeding on human renal extracellular matrix (hrECM). Comparison of hAFSC before and after seeding on hrECM *(A-B)*. It is evident by the Luminex analysis that hAFSC seeded on hrECM present high metabolic activity; cells secrete different molecules like Rantes, TNF-α and TNF-β. A general trend is noticeable: cells are very active within the first two weeks after seeding compared to cells before seeding. * = $p<0.05$; ** = $p<0.001$. For clarity of the data the multiple comparison between different time points and its statistical significance is reported in Table 2. Media was collected from 3 samples and analysis repeated in triplicate.

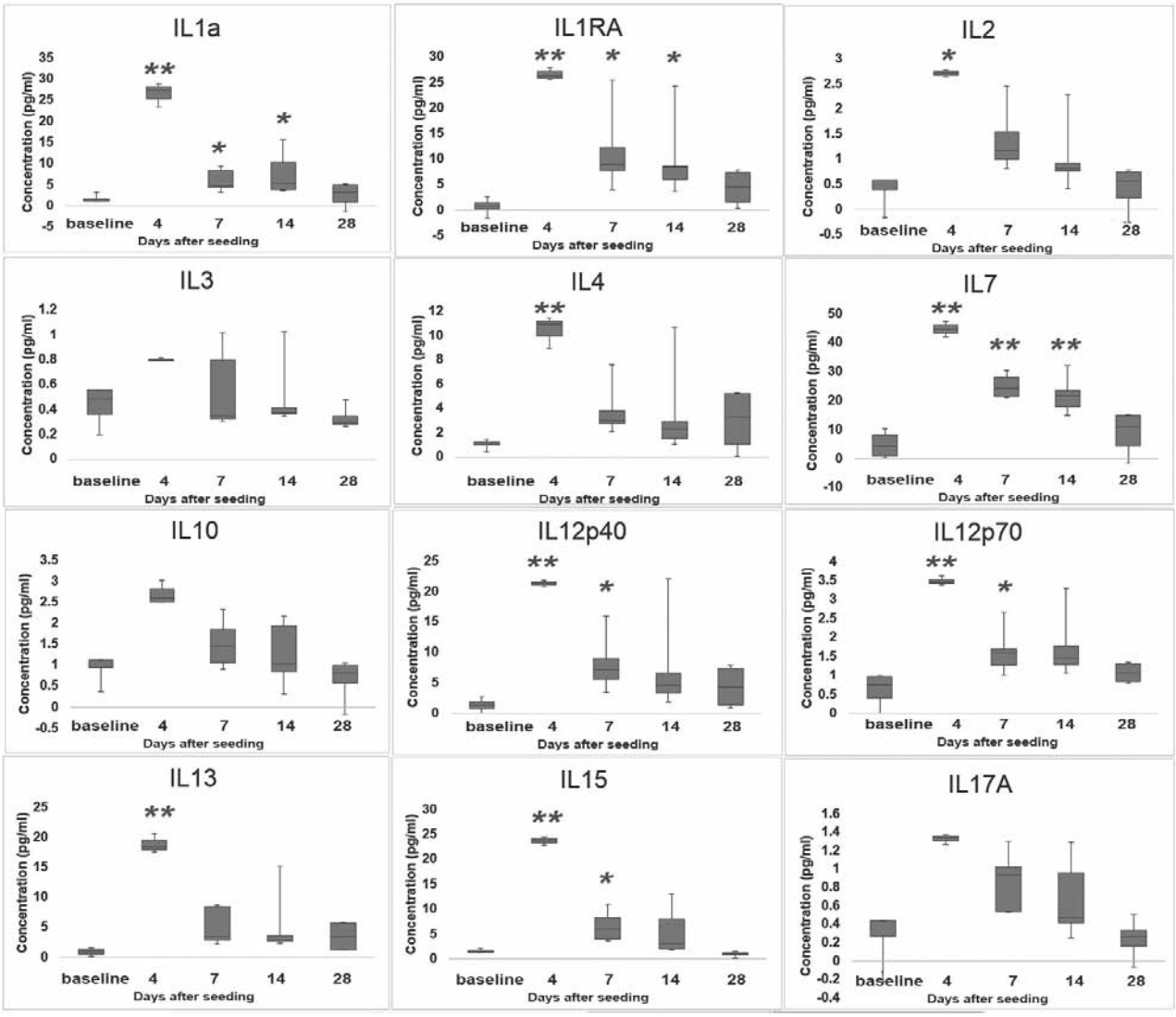


**Figure 4.** Secretome analysis demonstrated secretion of various cytokines by hAFSC over 4, 7, 14 and 28 days after seeding on human renal extracellular matrix (hrECM). Comparison of hAFSC before and after seeding on hrECM. It is evident by the Luminex analysis that hAFSC seeded on hrECM present high metabolic activity; cells secrete different molecules types of cytokines including IL1a, IL1Ra, IL12p40. A general trend is noticeable: cells are very active within the first two weeks after seeding compared to cells before seeding. * = $p<0.05$; ** = $p<0.001$. For clarity of the data the multiple comparison between different time points and its statistical significance is reported in Table 2. Media was collected from 3 samples and analysis repeated in triplicate.

### Cell proliferation and death (Figure 1).

In order to assess hAFSC proliferation and cell death, we performed immunohistochemical analysis for PCNA (proliferation) and BAX (apoptosis). On day 14, a high number of cells are present within the seeded matrix as shown by the PCNA staining (Figure 1B) and also confirmed by PCNA/BAX ratio as demonstrated (Figure 1I). On day 28, however, not only are less cells are visible, but they stain strongly positive for BAX in all renal comportments (Figure 1G), while the PCNA/BAX ratio flips in favor of apoptosis (Figure 1I). After 28 days in culture it was difficult to perform cell counting; the limitation of the *in vitro* culture setting (like for example absence of growth factors that might promote cellular survival or the use of more sophisticated bioreactors) might not allow to extend further life span of hAFSC on hrECM. Nevertheless, the survival of hAFSC on a hrECM for 28 days is already an evident improvement compared to available literature[1,3,4].

**Table 2. Summary of statistically significant variations in protein expression (secretome arrays discussed in Figure 5, 6 and 7) of hAFSC when seeded on hrECM at different time points (day 4, day 7, day 14 and day 28).**

| | | D4 vs D7 | D4 vs D14 | D4 vs D28 | D7 vs D14 | D7 vs D28 | D14 vs D 28 |
|---|---|---|---|---|---|---|---|
| Figure 5 | MMP-1 | | | | | | |
| | MMP-2 | | $p<0.05$ | $p<0.05$ | | $p<0.05$ | |
| | MMP-7 | $p<0.05$ | $p<0.05$ | $p<0.05$ | | | |
| | MMP-10 | | | | | | |
| | TIMP-1 | | | | | | |
| | TIMP-2 | $p<0.05$ | $p<0.05$ | $p<0.05$ | | | |
| | VEGF | $p<0.001$ | $p<0.001$ | $p<0.001$ | | | |
| | TGF-α | $p<0.05$ | $p<0.05$ | p<0.001 | | | |
| | IL6 | | | | | | |
| | IL8 | | $p<0.05$ | $p<0.001$ | | $p<0.001$ | $p<0.001$ |
| | PDGF-AA | $p<0.05$ | $p<0.001$ | $p<0.001$ | $p<0.05$ | $p<0.001$ | $p<0.001$ |
| | PDGF-BB | | | | | | |
| | IP10 | | | | | | |
| | **Comparison** | **D4 vs D7** | **D4 vs D14** | **D4 vs D28** | **D7 vs D14** | **D7 vs D28** | **D14 vs D 28** |
| Figure 6 | GM-CSF | $p<0.001$ | $p<0.001$ | $p<0.001$ | | | |
| | G-CSF | $p<0.001$ | $p<0.001$ | $p<0.001$ | | $p<0.05$ | |
| | MCP1 | | | | | | |
| | Fractalkine | $p<0.05$ | $p<0.05$ | $p<0.001$ | | $p<0.05$ | $p<0.05$ |
| | RANTES | $p<0.001$ | $p<0.001$ | $p<0.001$ | p<0.001 | $p<0.05$ | |
| | GRO-α | $p<0.001$ | $p<0.001$ | $p<0.001$ | $p<0.05$ | $p<0.001$ | $p<0.05$ |
| | TNF-α | $p<0.001$ | $p<0.001$ | $p<0.001$ | | | |
| | TNF-β | $p<0.05$ | $p<0.05$ | $p<0.001$ | | | $p<0.05$ |
| | MIP1b | | $p<0.05$ | $p<0.05$ | | | |
| | sCD40L | $p<0.05$ | $p<0.05$ | $p<0.05$ | | | |
| | MDC | $p<0.05$ | $p<0.05$ | $p<0.001$ | | | |
| | MCP3 | $p<0.05$ | $p<0.05$ | $p<0.001$ | | $p<0.05$ | $p<0.05$ |
| | INF-α2 | $p<0.05$ | $p<0.05$ | $p<0.05$ | | | |
| | INF-γ | $p<0.05$ | $p<0.05$ | $p<0.05$ | | | |
| | **Comparison** | **D4 vs D7** | **D4 vs D14** | **D4 vs D28** | **D7 vs D14** | **D7 vs D28** | **D14 vs D 28** |
| Figure 7 | IL1A | $p<0.001$ | $p<0.001$ | $p<0.001$ | | | |
| | IL1RA | | $p<0.05$ | $p<0.05$ | | $p<0.05$ | |
| | IL2 | | | $p<0.05$ | | | |
| | IL3 | | | | | | |
| | IL4 | $p<0.05$ | $p<0.05$ | $p<0.05$ | | | |
| | IL7 | $p<0.05$ | $p<0.05$ | $p<0.001$ | | $p<0.05$ | $p<0.05$ |
| | IL10 | | | $p<0.05$ | | | |
| | IL12p40 | | $p<0.05$ | $p<0.05$ | | | |
| | IL12p70 | $p<0.05$ | $p<0.05$ | $p<0.001$ | | | |
| | IL13 | $p<0.05$ | $p<0.05$ | $p<0.001$ | | | |
| | IL15 | $p<0.001$ | $p<0.001$ | $p<0.001$ | | | |
| | IL17A | | | | | | |

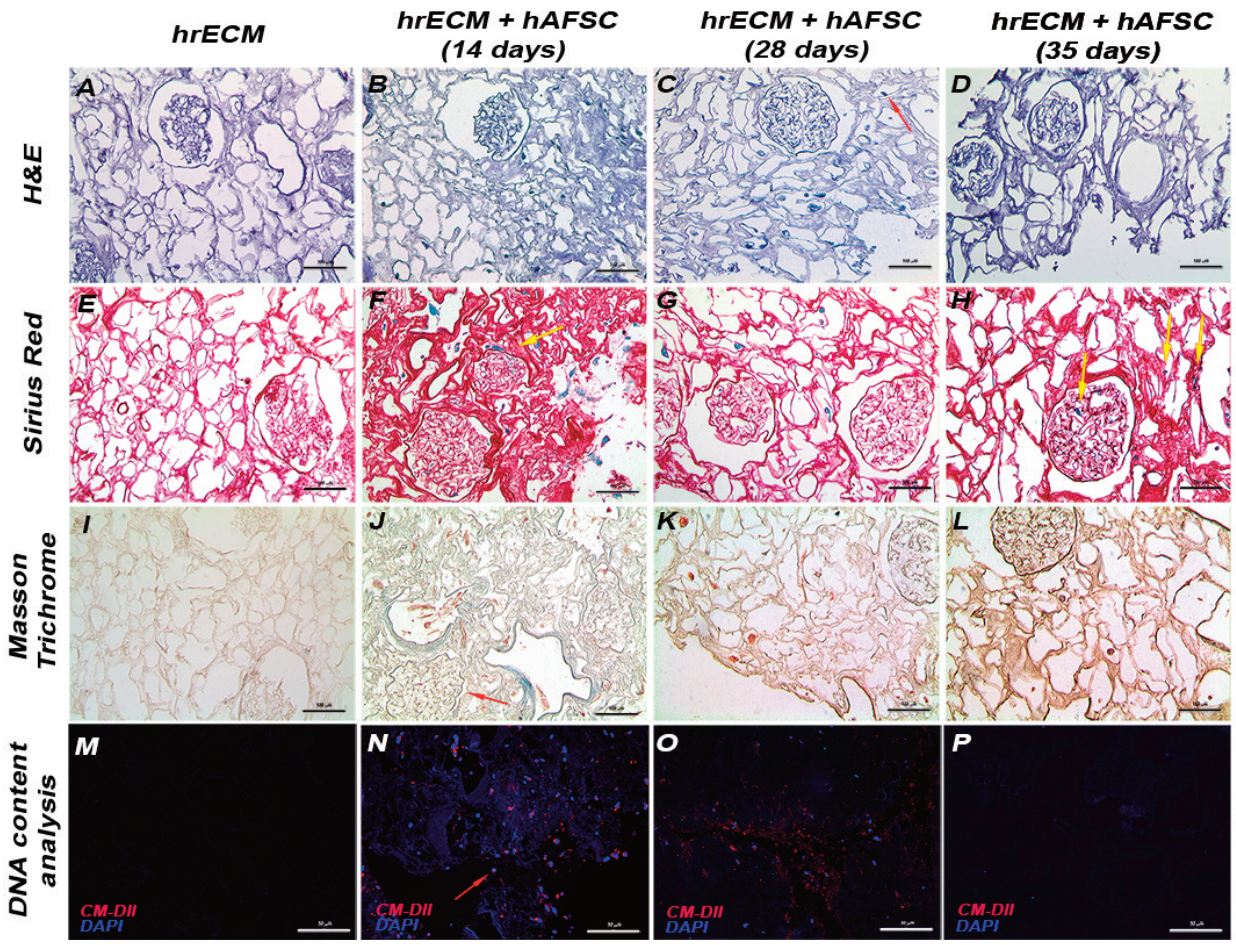


**Figure 5.** Histological analysis of hAFSC distribution over 14, 28, and 35 days after seeding on human renal extracellular matrix (hrECM). Representative bright field images of H&E *(A-D)*, Sirius Red *(E-H)*, Masson Trichrome *(I-L)* of hAFSC seeded on hrECM (*B-D, F-H J-L*) and hrECM alone (*A,E,I*). Discarded hrECM demonstrated noticeable accumulation of various fibrotic scars as shown in Figure *F*, arrow. hAFSC are detectable within different structures such as the glomerulus (*H*, *arrow*), the interstitial space (*C*, *arrow*). M-P are representative immune fluorescence DAPI staining of seeded cells. In Figure N it is evident the presence of hAFSC labeled with CM-Dil (red fluorescence, nuclei is stained with DAPI, arrow). *A-L*: scale bar: 100 μm; M-P: scale bar: 50 μm.

### Transmission electronic microscopy (TEM) evaluation of seeded hrECM (Figure 6).

To assess ultrastructural morphology of seeded hrECM, the samples were studied with TEM before seeding and at day 28 post seeding with hAFSC. Presence of cells in all the different compartments of the decellularized kidney was assessed by histological analysis (H&E) of ultra-thin epoxy resin samples; after 28 days hAFSC were localized in all the renal compartments including glomeruli and interstitial space (Figure 6A). As previously described[13], acellular hrECM present a well preserved ultrastructure of the glomerular basement membrane (Figure 6B). Ultrastructure analysis confirmed that cells acquire a specific morphology based on their integration in glomerulus (Figure 6C-D), tubules (Figure 6E), interstitium (Figure 6F) and capillaries (Figure 6G), where for example hAFSC assume an elongated shape in the interstitial space compared to a more rounded morphology in the glomerulus. These results might suggest high plasticity and ability to adapt to the different decellularized renal compartments. Moreover, after 28 days, hAFSC seeded on hrECM show signs of functional activity; TEM revealed extensive expression of Golgi apparatus, endoplasmic reticulum, secretory granules and vacuoles within the cells: indicative of cellular activity and secretion and a normal nuclear morphology (Figure 6C-G). Interestingly, multiple junctions were observed between the cells and the matrix (Figure 6D). These findings are of great relevance as junctions are essential for intra- and inter-cellular signaling, and ultimately for cell proliferation, apoptosis and differentiation[21].

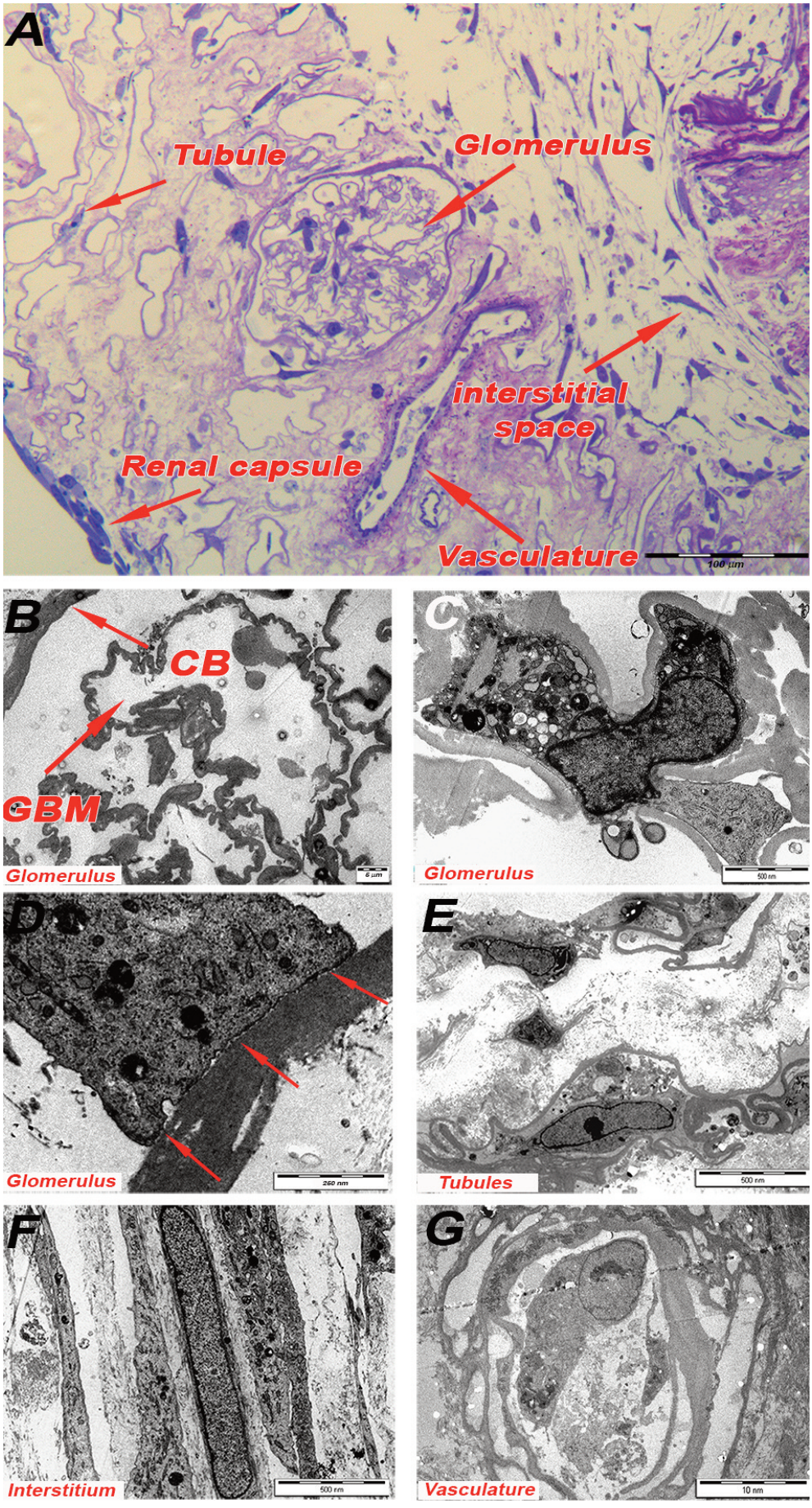


**Figure 6.** Evaluation of cell morphology by H&E and transmission electron microscopy of hAFSC after 28 days after seeding on human renal extracellular matrix (hrECM). Morphological analysis of ultra-thin epoxy resin samples of cells seeded onto decellularized matrix after 28 days confirmed the presence of cells in all the distinct compartments of the renal ECM. Interestingly, cells acquired a specific morphology depending on their localization within the decellularized matrix, like glomerulus, vasculature, tubules, interstitial space and renal capsule (*A*, *arrows*, 20X). TEM analysis of samples after decellularization, confirms that hrECM ultrastructures are preserved *(B)*; capsule of Bowman, CB, and glomerular basement membrane, GBM (*arrows*) maintain their structure. Moreover, TEM analysis confirmed the vastly diverse morphological ultrastructure of cells localized within the glomerular compartment with formation of junctions between hAFSC and the matrix (*C*, *arrows*; *D*), tubules *(E)*, interstitial space *(F)* and vasculature *(G)*. Independently from their localization, all cells showed a marked expression of endoplasmic reticulum and Golgi apparatus, along with multiple secretory granules and vacuoles and normal nuclear morphology.

### hrECM induce the expression of genes of kidney development (Figure 7).

To determine whether hrECM are able to induce renal differentiation by hAFSC, we evaluated the expression of different genes involved in kidney development as well as markers expressed in mature renal cells such as Wilms tumor WT-1, PAX2, LMX1B, glial cell derived neurotrophic factor GDNF, podocalyxin like-2, nephrin and synaptopodin like-2 (Table 1). mRNA was collected from represent pooled of 6 samples for hAFSC after seeding and for hrECM alone. PCR was repeated in triplicate for all experimental groups, including hAFSC before seeding.

The vital early kidney developmental markers PAX2 and LMX1B were newly expressed after 14 days of seeding (Figure 7A), while WT1, GDNF and podocalyxin like-2 were expressed by hAFSC before seeding (Figure 7C). Later developmental markers such as nephrin and synaptopodin like-2 were not expressed, not even at day 28. Importantly, as hAFSC were not cultured in any specific renal differentiation media, we can speculate that the matrix itself is able to guide hAFSC differentiation towards a renal lineage commitment, in agreement with previously reported observations by Remuzzi's group[11].

### hAFSC seeded on hrECM secrete various proteins

Luminex analysis was conducted on media harvested from samples of hAFSC seeded on hrECM at day 4, 7, 14 and 28 days. Significance of expression ($p^*<0.05$, $p^*<0.001$) was determined through the comparison of the secretion of various proteins (like VEGF, MMPs, TIMPs, etc.) by hAFSC before and after seeding on hrECM (Figures 2, 3 and 4) and also between different time points (Table 2).

Luminex analysis demonstrated secretion of various MMPs and TIMPs in the media collected from seeded hrECM (Figure 2A-B, Table 2). In the study group, secretion of MMP-2 and MMP-7 in the media began early after seeding, peaked on day 4, but dropped to baseline levels from the second week onward (Figure 2A); MMP-1 was not highly expressed. TIMPs, which are modulators of MMPs, were also expressed significantly alongside MMPs. In the study group, TIMP synthesis and release in the culture media occurred very early, peaked on day 4, remained significant through day 7, but dropped thereafter (Figure 2B, Table 2). Moreover, TIMP-2 expression correlated with MMP-2 expression. Importantly, both MMP-2 and TIMP-2 are highly expressed when compared to the cells before seeding thus indicating that cells are stimulated by the hrECM to induce expression of matrix modulators.

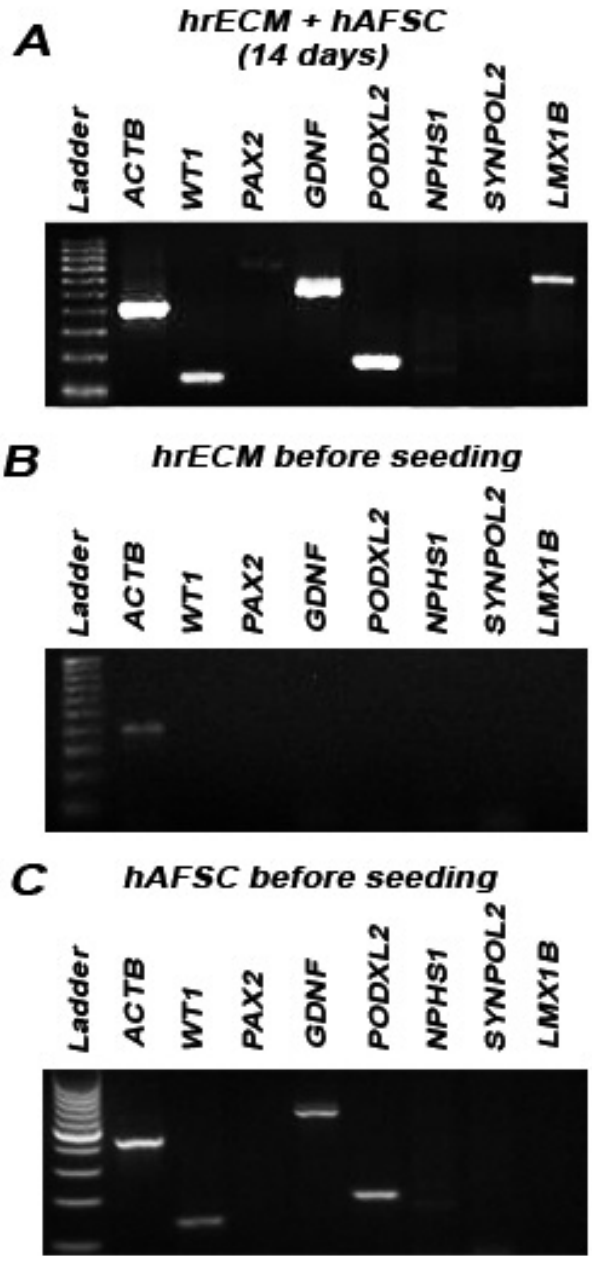


**Figure 7.** Analysis of hAFSC on hrECM on day 14 revealed expression of early renal markers. WT1, GDNF, podocalyxin like-2, Pax 2, and LMX1B were expressed by hAFSC seeded on hrECM after 14 days *(A)*, while hrECM alone did not show any expression of renal genes *(B)*. hAFSC before seeding expressed GDNF, WT1, Pax2 and podocalyxin like-2 *(C)*. Nephrin and synaptopodin like-2 were not expressed by hAFSC before or after seeding on hrECM. β-actin is used as housekeeping gene. mRNA was collected from represent pooled of 6 samples for hAFSC after seeding and for hrECM alone. PCR was repeated in triplicate for all experimental groups, including hAFSC before seeding.

Growth factors such as VEGF and TGF-α are key players in different tissue remodeling processes, including angiogenesis. On day 4, hAFSC in hrECM express high levels of VEGF and TGF-α compared to hAFSC prior to seeding (Figure 2C). Furthermore, hAFSC show high activity at day 4 for IL8 and PDGF-AA when seeded on hrECM; this expression decreases overtime as shown in Table 2. Expression of VEGFA by hAFSC was also confirmed by mRNA (Figure 5D), showing that hrECM induces high stimulation of this particular growth factor.

Numerous chemokines could also be detected in the culture media, at significant concentrations and at different time points (Figure 3A-B, Table 2). In particular, growth-regulated oncogene (GRO), which, like many other cytokines, is involved in multiple processes including inflammation, angiogenesis, wound healing, tumor invasion, and metastasis[22], was highly expressed by hAFSC seeded on hrECM on day 4 and day 7 compared to hAFSC before seeding. Significant elevation in the expression of granulocyte colony-stimulating factor (G-CSF) and granulocyte-macrophage colony-stimulating factor (GM-CSF) was also observed in hAFSC in hrECM on day 4 in comparison to hAFSC before seeding. In addition, TNF-α, a well-known activator of angiogenesis, was highly expressed on day 4 but dropped drastically thereafter. Finally, as shown in Figure 4 and Table 2, hrECM induces high levels of different cytokines such as IL1a, IL1Ra and IL12p40, especially during the first week after seeding.

Altogether, these data provide evidence that, when seeded on hrECM, hAFSC are functionally active, as demonstrated by their ability to synthesize key molecules involved in critical pathways for tissue and organ homeostasis such as inflammation, angiogenesis and matrix remodeling.

## Discussion

In organ bioengineering and regeneration, the seeding of specific cell types on acellular ECM scaffolds produced from animal or human organs seems to offer the quickest route to clinical application. Thus far, numerous studies from different laboratories have produced interesting data mainly from non-clinically relevant animal models[23], yet the production of a fully regenerated and functional bioengineered complex organ such as the kidney has yet to be reported. As the technology currently stands, numerous obstacles need to be overcome before a viable and functioning kidney-like structure can be manufactured and transplanted into patients. These include the inadequate understanding of the mechanisms of interaction between ECM and cells, and the choice of cell type to use to reconstitute the cellular compartment of acellular scaffolds[1,3]. The innate ECM in disease, development, and healthy tissue exhibits a dynamic interplay of biochemistry and three-dimensional architecture. Hence, the utilization of ECM as a biomaterial may facilitate the engineering of a "human bioactive system" for directing cellular behavior and function.

As highlighted in the introduction, our study builds on successful previous investigations demonstrating that hrECM obtained from discarded kidneys may represent an ideal platform for kidney bioengineering and regeneration[13]. In this work, we established an *in vitro* model with which, by seeding stem cells on sections of hrECM, we aimed to assess a) cellular adhesion and viability and b) cellular function and metabolic activity. The study was designed to specifically address the effect of matrices on stem cell biology and did not focus primarily on the repopulation of hrECM nor the determination of renal lineage commitment by stem cells. Thus, cells were seeded at a defined concentration and not by any inducible renal differentiation media. Notably, the choice to use hAFSC was made due to their ability to modulate disease progression in both acute and chronic kidney diseases[15,16], as well as to release different growth factors (e.g. VEGF), cytokines, and matrix modeling proteins including MMPs and TIMPs[19], which are essential in kidney remodeling and regeneration. Importantly, no study has described how a decellularized matrix can influence the secretome profile of stem cells. Investigating the role of ECM in changing the protein secretion of stem cells while transitioning from a basic two-dimensional culture to a relevant three-dimensional culture system may contribute to the improvement of tissue engineering in the near future.

Our data demonstrate that hrECM seeded with hAFSC behave as a "biosystem" wherein cells attach and proliferate throughout the 3D framework of the matrix. Functionally, cells are extremely active as demonstrated by their ability to synthesize and release into the environment numerous growth factors, chemokines, and cytokines (Figures 2 to 4, Table 2). *In vivo*, it is well known that during a regeneration process, important molecular signaling pathways are strongly activated[24]. For example, angiogenic inducers such as VEGF, TGF-α, and platelet-derived growth factors (PDGF) are upregulated which induces neo-angiogenesis[25,26]. hAFSC secrete these factors at a high level, especially dur-

ing the first two weeks after seeding. It is reasonable to speculate that hrECM are capable of inducing hAFSC to release these factors, especially when we compare the secretome profile of hAFSC in a two-dimensional culture before seeding. Importantly, hAFSC are highly stimulated to produce a variety of interleukins such as IL-6, IL-1, and IL-1ra which are involved in different regeneration processes[27,28] as well as chemokine signaling molecules such as G-CSF and GM-CSF which are involved in the recruitment and activation of endogenous cells[29] during organ repair.

Importantly, MMPs are secreted or anchored to the cell surface, and exert a myriad of functions spanning from the control of the homeostasis of ECM to the regulation of the innate immune response and numerous other pathways. They do so via the mobilization of growth factors and/or the cleavage and release of cytokines, chemokines, surface proteins, and receptors[30]. In addition to their inhibitory role against most of the known MMPs, TIMPs promote cell proliferation in a wide range of cell types, have shown anti-apoptotic function, and are synthesized in response to several different cytokines and hormones[28,31] TIMPs are critical to the maintenance of tissue homeostasis by suppressing the proliferation of quiescent tissues in response to angiogenic factors, and by inhibiting protease activity in tissues undergoing remodeling of the ECM[28,31]. Induction of signals for ECM turnover by hAFSC secretion was observed through production of MMPs and TIMPs during the first 2 weeks after the seeding. Notably, the activity of MMP-2 is correlated with TIMP-2 and TIMP-1 as it is during various phases of renal development[32].

In our biosystem, cells were extremely active immediately after seeding and their proliferative and synthetic capacities peaked during the second week post-seeding. On the contrary, from the beginning of the 3rd week, secretory and proliferative capacity degraded to an eventual nadir at the end of the study period. These findings are possibly explained by the low number of cells that we used for our seeding experiments and by the adopted culture conditions, which did not include a dynamic perfusion system since the purpose of the present study was not, in fact, to achieve full repopulation of the scaffolds. Lastly, we also concluded that hrECM were able to stimulate hAFSC toward renal lineage commitment because the cells were able to induce the expression of two important renal developmental genes, Pax2 and LMX1B after 14 days of seeding, even though they were cultured in basic media without the addition of renal stimulation lineage commitment factors. This result is very intriguing because it underscores the capabilities of matrix alone in guiding renal stem cell differentiation.

## Conclusions

This is the first study describing the long-term culture of stem cells seeded on hrECM. The significant increase in the secretion of growth, hematopoietic, angiogenic, and extracellular remodeling proteins suggests an innate remodeling response in hAFSC during the initial interaction with discarded kidney extracellular matrix. Our model provides critical information which may be of importance in both kidney bioengineering and regeneration, as well as repair given the characteristics of our matrix.

## Acknowledgements

We thank Dr H. Shimada and Minerva Mongeotti for the help with the transmission electron microscopy (TEM) protocols and interpretation of the data. We thank Dr R. Habibian for kindly providing the amniotic fluid samples. We thank the California Institute for Regenerative Medicine (CIRM, Da Sacco S and Sedrakyan S) and the GOFFAR Foundation for financial support (Perin L). Andrea Peloso, MD, received a grant from the Fondazione Banca del Monte di Lombardia – Progetto Professionalità Ivano Becchi. We acknowledge Carolina Donor Services and LifeShare of the Carolinas for their invaluable support.

## Conflict of Interest

The Authors declare no conflict of interest.

## Reference

1. Orlando G, Soker S, Stratta RJ. Organ bioengineering and regeneration as the new Holy Grail for organ transplantation. Ann Surg 2013; 258(2): 221-232.
2. Lechler RI, Sykes M, Thomson AW, Turka LA. Organ transplantation--how much of the promise has been realized? Nat Med 2005; 11(6): 605-613.
3. Badylak SF, Taylor D, Uygun K. Whole-organ tissue engineering: decellularization and recellularization of three-dimensional matrix scaffolds. Annu Rev Biomed Eng 2011; 13: 27-53.
4. Cortiella J, Niles J, Cantu A, Brettler A, Pham A, Vargas G, Winston S, Wang J, Walls S, Nichols JE. Influence of acellular natural lung matrix on murine embryonic stem cell differentiation and tissue formation. Tissue Eng Part A 2010; 16(8): 2565-2580.

5. Ahn EH, Kim Y, Kshitiz, An SS, Afzal J, Lee S, Kwak M, Suh KY, Kim DH, Levchenko A. Spatial control of adult stem cell fate using nanotopographic cues. Biomaterials 2014; 35(8): 2401-2410.
6. Biggs MJ, Richards RG, Dalby MJ. Nanotopographical modification: a regulator of cellular function through focal adhesions. Nanomedicine 2010; 6(5): 619-633.
7. Teti A. Regulation of cellular functions by extracellular matrix. J Am Soc Nephrol 1992; 2(10 Suppl): S83-87.
8. Orlando G, Farney AC, Iskandar SS, Mirmalek-Sani SH, Sullivan DC, Moran E, AbouShwareb T, De Coppi P, Wood KJ, Stratta RJ, Atala A, Yoo JJ, Soker S. Production and implantation of renal extracellular matrix scaffolds from porcine kidneys as a platform for renal bioengineering investigations. Ann Surg 2012; 256(2): 363-370.
9. Nakayama KH, Lee CC, Batchelder CA, Tarantal AF. Tissue specificity of decellularized rhesus monkey kidney and lung scaffolds. PLoS One 2013; 8(5): e64134.
10. Ng SL, Narayanan K, Gao S, Wan AC. Lineage restricted progenitors for the repopulation of decellularized heart. Biomaterials 2011; 32(30): 7571-7580.
11. Bonandrini B, Figliuzzi M, Papadimou E, Morigi M, Perico N, Casiraghi F, Dipl C, Sangalli F, Conti S, Benigni A, Remuzzi A, Remuzzi G. Recellularization of well-preserved acellular kidney scaffold using embryonic stem cells. Tissue Eng Part A 2014; 20(9-10): 1486-1498.
12. Wang Y, Cui CB, Yamauchi M, Miguez P, Roach M, Malavarca R, Costello MJ, Cardinale V, Wauthier E, Barbier C, Gerber DA, Alvaro D, Reid LM. Lineage restriction of human hepatic stem cells to mature fates is made efficient by tissue-specific biomatrix scaffolds. Hepatology 2011; 53(1): 293-305.
13. Orlando G, Booth C, Wang Z, Totonelli G, Ross CL, Moran E, Salvatori M, Maghsoudlou P, Turmaine M, Delario G, Al-Shraideh Y, Farooq U, Farney AC, Rogers J, Iskandar SS, Burns A, Marini FC, De Coppi P, Stratta RJ, Soker S. Discarded human kidneys as a source of ECM scaffold for kidney regeneration technologies. Biomaterials 2013; 34(24): 5915-5925.
14. Perin L, Sedrakyan S, Da Sacco S, De Filippo R. Characterization of human amniotic fluid stem cells and their pluripotential capability. Methods Cell Biol 2008; 86: 85-99.
15. Perin L, Sedrakyan S, Giuliani S, Da Sacco S, Carraro G, Shiri L, Lemley KV, Rosol M, Wu S, Atala A, Warburton D, De Filippo RE. Protective effect of human amniotic fluid stem cells in an immunodeficient mouse model of acute tubular necrosis. PLoS One 2010; 5(2): e9357.
16. Sedrakyan S, Da Sacco S, Milanesi A, Shiri L, Petrosyan A, Varimezova R, Warburton D, Lemley KV, De Filippo RE, Perin L. Injection of amniotic fluid stem cells delays progression of renal fibrosis. J Am Soc Nephrol 2012; 23(4): 661-673.
17. De Coppi P, Bartsch G, Jr., Siddiqui MM, Xu T, Santos CC, Perin L, Mostoslavsky G, Serre AC, Snyder EY, Yoo JJ, Furth ME, Soker S, Atala A. Isolation of amniotic stem cell lines with potential for therapy. Nat Biotechnol 2007; 25(1): 100-106.
18. Carraro G, Perin L, Sedrakyan S, Giuliani S, Tiozzo C, Lee J, Turcatel G, De Langhe SP, Driscoll B, Bellusci S, Minoo P, Atala A, De Filippo RE, Warburton D. Human amniotic fluid stem cells can integrate and differentiate into epithelial lung lineages. Stem Cells 2008; 26(11): 2902-2911.
19. Garcia O, Carraro G, Turcatel G, Hall M, Sedrakyan S, Roche T, Buckley S, Driscoll B, Perin L, Warburton D. Amniotic fluid stem cells inhibit the progression of bleomycin-induced pulmonary fibrosis via CCL2 modulation in bronchoalveolar lavage. PLoS One 2013; 8(8): e71679.
20. Villani V, Milanesi A, Sedrakyan S, Da Sacco S, Angelow S, Conconi MT, Di Liddo R, De Filippo R, Perin L. Amniotic fluid stem cells prevent beta-cell injury. Cytotherapy 2014; 16(1): 41-55.
21. Osanai M. The tight junction, intercellular seal as a cell signaling player: protocols for examination of its status. Methods Mol Biol 2011; 762: 43-62.
22. Keglowich L, Roth M, Philippova M, Resink T, Tjin G, Oliver B, Lardinois D, Dessus-Babus S, Gosens R, Hostettler Haack K, Tamm M, Borger P. Bronchial smooth muscle cells of asthmatics promote angiogenesis through elevated secretion of CXC-chemokines (ENA-78, GRO-alpha, and IL-8). PLoS One 2013; 8(12): e81494.
23. Song JJ, Guyette JP, Gilpin SE, Gonzalez G, Vacanti JP, Ott HC. Regeneration and experimental orthotopic transplantation of a bioengineered kidney. Nat Med 2013; 19(5): 646-651.
24. DuBuc TQ, Traylor-Knowles N, Martindale MQ. Initiating a regenerative response; cellular and molecular features of wound healing in the cnidarian Nematostella vectensis. BMC Biol 2014; 12: 24.
25. Dong A, Seidel C, Snell D, Ekawardhani S, Ahlskog JK, Baumann M, Shen J, Iwase T, Tian J, Stevens R, Hackett SF, Stumpp MT, Campochiaro PA. Antagonism of PDGF-BB suppresses subretinal neovascularization and enhances the effects of blocking VEGF-A. Angiogenesis 2014; 17(3): 553-562.
26. Westphal JR, Van't Hullenaar R, Peek R, Willems RW, Crickard K, Crickard U, Askaa J, Clemmensen I, Ruiter DJ, De Waal RM. Angiogenic balance in human melanoma: expression of VEGF, bFGF, IL-8, PDGF and angiostatin in relation to vascular density of xenografts in vivo. Int J Cancer 2000; 86(6): 768-776.
27. Leibinger M, Muller A, Gobrecht P, Diekmann H, Andreadaki A, Fischer D. Interleukin-6 contributes to CNS axon regeneration upon inflammatory stimulation. Cell Death Dis 2013; 4: e609.
28. Ueda T, Sakabe T, Oka M, Maeda Y, Nishida M, Murakami F, Maekawa T. Levels of interleukin (IL)-6, IL-8, and IL-1 receptor antagonist in the hepatic vein following liver surgery. Hepatogastroenterology 2000; 47(34): 1048-1051.
29. Sohn SK, Kim JG, Seo KW, Chae YS, Jung JT, Suh JS, Lee KB. GM-CSF-based mobilization effect in normal healthy donors for allogeneic peripheral blood stem cell transplantation. Bone Marrow Transplant 2002; 30(2): 81-86.
30. Chen P, Parks WC. Role of matrix metalloproteinases in epithelial migration. J Cell Biochem 2009; 108(6): 1233-1243.
31. Stetler-Stevenson WG. Tissue inhibitors of metalloproteinases in cell signaling: metalloproteinase-independent biological activities. Sci Signal 2008; 1(27): re6.
32. Legallicier B, Trugnan G, Murphy G, Lelongt B, Ronco P. Expression of the type IV collagenase system during mouse kidney development and tubule segmentation. J Am Soc Nephrol 2001; 12(11): 2358-2369.